Journal of Power Sources 208 (2012) 237–241

Contents lists available at SciVerse ScienceDirect

Journal of Power Sources

journal homepage: www.elsevier.com/locate/jpowsour

Short communication

Influence of lithium content on the electrochemical performance of $Li_{1+x}(Mn_{0.533}Ni_{0.233}Co_{0.233})_{1-x}O_2$ cathode materials

Zhaohui Tang, Zhixing Wang*, Xinhai Li, Wenjie Peng

School of Metallurgical Science and Engineering, Central South University, Changsha 410083, China

ARTICLE INFO

Article history:
Received 17 December 2011
Received in revised form 17 February 2012
Accepted 20 February 2012
Available online 3 March 2012

Keywords:
Cathode
Lithium-ion batteries
Rate capability
Cycle performance

ABSTRACT

Li-rich Mn-based $Li_{1+x}(Mn_{0.533}Ni_{0.233}Co_{0.233})_{1-x}O_2$ (x = 0, 0.045, 0.09, 0.135, 0.18, 0.225) materials have been prepared by a conventional solid-state reaction. XRD, SEM and half-cell tests are investigated on the influence of Li content. Pure phase can be obtained when Li-excessive value x keeps between 0.045 and 0.18. The initial efficiency (Q_{1d}/Q_{1c}) almost keeps the same level of 70% for different Li-excessive samples. $Li_{1.045}Mn_{0.509}Ni_{0.223}Co_{0.223}O_2$ sample shows highest discharge capacity of 259.8 mA h g^{-1}. $Li_{1.09}Mn_{0.486}Ni_{0.212}Co_{0.212}O_2$ sample exhibits the best rate capability, and almost no reduction is observed after 24-time cycles in different discharge current density.

1. Introduction

Lithium-ion batteries are widely used in electronic devices, power sources, etc., due to their light weight, high-energy density, and long cycle life. Cathode materials are combined from transition metal elements Co, Mn and Ni or their complicated compounds. $LiCoO_2$ or $LiNi_{1/3}Mn_{1/3}Co_{1/3}O_2$ has excellent electrochemical performance, but deficient in Co resources and poor in safety performance. $LiMn_2O_4$ exhibits the virtue of low cost, rich resources and high safety. However, dissolution of Mn and Jahn–Teller effect make the long-life cycle performance poor. $LiFePO_4$ can be used for large-scale application but demand of further enhancement of the energy density of the rechargeable batteries is urgent. Recently, series layered Li-rich Mn-based materials become one of the research focuses for their low cost, high capacity and long cycle life under high-voltage charge–discharge condition.

Among the Li-rich Mn-based cathode materials reported so far, Mn–Ni–Co system is seemed to be the most promising candidates and being studied mostly. Guo et al. systematically studied $yLi(Li_{1/3}Mn_{2/3})O_2\cdot(1-y)Li(Ni_{1/3}Mn_{1/3}Co_{1/3})O_2$ ($0 \le x \le 0.9$) materials through structural and electrochemical characterization, a high capacity of 250 mA h g^{-1} (y = 0.6) can be obtained [1]. To optimize the energy density and cycle ability, researches of the different ratio between Li_2MnO_3 and $Li[Ni_{1/3}Mn_{1/3}Co_{1/3}]O_2$ were been carried out [2–4]. Characterized as the chemical formula of $Li[Li_xMn_yNi_zCo_{1-x-y-z}]O_2$, many Li-rich Mn-based materials have also been widely studied [5–7]. Methods such as metal oxide surface modification or Li–Ni–PO_4 treatment was employed to improve initial irreversible capacity and rate capability [8,9]. However, little work focus on Mn:Ni:Co = 0.533:0.233:0.233 systems and influence of lithium content. Santhanam and co-workers investigated the relationship between lithium content and rate cycle ability of $Li_{1+x}Ni_{0.30}Ni_{0.30}Mn_{0.40}O_2$ [10] but not on 0.533:0.233:0.233 systems; furthermore, the voltage range employed was relatively low of 2.5–4.3 V for high-energy density character of Li-rich Mn-based materials.

In order to keep the Mn content and equilibrium of Ni and Co, which both for high-capacity and structure stability, so that idea solid solution $yLi_2MnO_3\cdot(1-y)LiNi_{1/3}Mn_{1/3}Co_{1/3}O_2$ with novelty can be obtained. In this paper, we aim at Mn:Ni:Co = 0.533:0.233:0.233 systems and through systemic optimization of Li content to synthesize $Li_{1+x}(Mn_{0.533}Ni_{0.233}Co_{0.233})_{1-x}O_2$ cathode materials. XRD, SEM and half-cell tests were investigated on the influence of Li content on characteristics of structure, morphology and electrochemical properties.

2. Experiment

Materials were prepared by a conventional solid-state reaction using lithium carbonate and the metal hydroxide with Mn:Ni:Co of 0.533:0.233:0.233 in the mol ratio. The x value of $Li_{1+x}(Mn_{0.533}Ni_{0.233}Co_{0.233})_{1-x}O_2$ selected is 0, 0.045, 0.09, 0.135, 0.18 and 0.225, referring to code A, B, C, D, E and F correspondingly.

* Corresponding author. Tel.: +86 018684675178; fax: +86 0731 88836633.
E-mail address: tangzh106@163.com (Z. Wang).

0378-7753/$ – see front matter © 2012 Elsevier B.V. All rights reserved.
doi:10.1016/j.jpowsour.2012.02.085

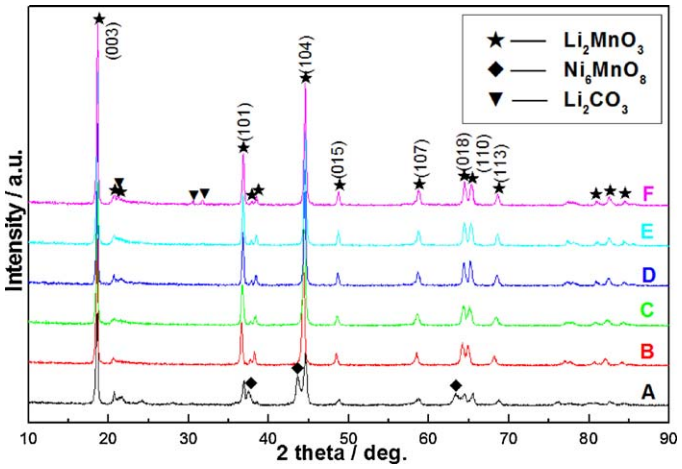

Fig. 1. XRD patterns of $Li_{1+x}(Mn_{0.533}Ni_{0.233}Co_{0.233})_{1-x}O_2$ samples (A, B, C, D, E, E referring to samples of $x = 0$, 0.045, 0.09, 0.135, 0.18, 0.225).

The materials were synthesized from lithium carbonate and metal hydroxide taken in stoichiometric quantities as the following procedure. (1) All ingredients were mixed for 3 h by ball-milling. (2) The mixture was calcinated at 850 °C in air for 20 h, and then cooled naturally. To find an optimized ratio, all the samples were compared with a fixed calcination condition.

Powder X-ray diffraction (XRD, Rint-1000, Rigaku, Japan) using Cu Kα radiation was employed to identify the crystalline phase of the synthesized materials. XRD data were obtained ($2\theta = 10$–$90°$) with a step size of 0.02°. The lattice parameters were calculated by the Rietveld method with General Structure Analysis Software (GSAS program, Los Alamos National Laboratory, USA). The particle size and morphology were measured by scanning electron microscopy (SEM, JSM6380LV) with an accelerating voltage of 20 kV. The compositions in terms of transition metal contents in the materials were analyzed by the inductively coupled plasma (ICP, Thermo Electron Corporation). The measured composition of the as-prepared materials is close to the target composition so that the nominal compositions are used to describe the materials throughout this paper for simplicity.

The electrochemical characterizations were performed using CR2430 coin cells. For positive electrode fabrication, the prepared materials were mixed with 5% of carbon black and 5% of polyvinylidene fluoride (PVDF) in N-methyl pyrrolidinone (NMP) solvent until the slurry was obtained. The blended slurries were pasted onto an aluminum current collector, and the electrode was dried at 120 °C for 12 h in the air, then electrode pieces were cut to 16 mm in diameter. The test cell consisted of the positive electrode and lithium foil negative electrode separated by a porous polypropylene film, and a mole L^{-1} $LiPF_6$ in EC and DMC (1:1 in volume) as the electrolyte. The assembly of the cells was carried out in a dry Ar-filled gloved box. The test was carried out using an automatic galvanostatic charge–discharge unit NEWWARE battery cycler between 2.0 and 4.8 V of charge–discharge voltage range. Different discharge current density of 20, 40, 100 and 200 mA g^{-1} versus Li/Li^+ electrodes at room temperature were tested, which cycled 6-times for each constant current density then turned to higher thus 24-time cycles were tested in all. The charge current density keeps in 20 mA g^{-1} in the initial six-time cycles, and then keeps in 40 mA g^{-1} in later 18-time cycles.

3. Results and discussion

Fig. 1 shows the powder XRD patterns of the synthesized $Li_{1+x}(Mn_{0.533}Ni_{0.233}Co_{0.233})_{1-x}O_2$ ($x = 0$, 0.045, 0.09, 0.135, 0.18, 0.225) materials. A metal oxide impurity of Ni_6MnO_8 is found in nominal $LiMn_{0.533}Ni_{0.233}Co_{0.233}O_2$ ($x = 0$), indicating that Li amount is not abundant in reacting process. The result is quite different from assay reported. The main reason is that compared to $LiMn_{0.4}Ni_{0.3}Co_{0.3}O_2$ material, our $LiMn_{0.533}Ni_{0.233}Co_{0.233}O_2$ sample exhibit higher Mn content, so more Li_2MnO_3 will be formed and more Li is needed based on stoichiometric quantities. At the same time, residual Li_2CO_3 is observed in Li excessive in 0.225, which maybe account for the Li-excessive keeps equal or lesser than 0.2 mostly [11,12].

Table 1
The lattice parameters of $Li_{1+x}(Mn_{0.533}Ni_{0.233}Co_{0.233})_{1-x}O_2$ samples.

x	a (Å)	c (Å)	c/a	V (Å^3)
0.045	2.8495	14.2236	4.9916	99.8994
0.090	2.8512	14.2258	4.9894	100.0341
0.135	2.8530	14.287	4.9873	100.1809
0.180	2.8546	14.2322	4.9857	100.3180

On the other hand, when Li-excessive value x keeps between 0.045 and 0.18, pure phase can be obtained and all the diffraction peaks can be indexed as a layered oxide structure based on a hexagonal α-$NaFeO_2$ structure. The small diffraction peaks between 20° and 23° are considered to be characteristic peaks of Li_2MnO_3-like or Li_2MnO_3-based materials. Although all observed XRD peaks in each sample can be indexed only by monoclinic unit cell of Li_2MnO_3 (C2/m), some of main XRD peaks can overlap the peak of position from the unit cell of cubic rock-salt structure (Fm3m). The materials show a (0 0 3) peak at $2\theta = 18.5°$ as a main peak, and (1 0 4), (1 0 1), (0 1 5), (1 0 7), (0 1 8), (1 1 0), (1 1 3) planes observed at $2\theta = 45°$, 37°, 48.5°, 58.5°, 64.5°, 65.5°, 68.5° peaks respectively, also clearly demonstrate the characteristic XRD peaks of the hexagonal structure. It can be found that split of (0 1 8) and (1 1 0) peaks are all obviously, implying well crystalline. Therefore, the as prepared materials exhibit a pure phase, which can be simply represented as $Li_{1+x}(Mn_{0.533}Ni_{0.233}Co_{0.233})_{1-x}O_2$ or composite solid solution $yLi_2MnO_3{\cdot}(1-y)LiNi_{1/3}Mn_{1/3}Co_{1/3}O_2$. Table 1 shows the lattice parameters and c/a ratios of as-prepared pure phase samples calculated by XRD data. It can be found that the lattice parameters a, c and V have increased but c/a decreased with the increase of Li excessive slightly, which is related to the bigger ion radius of Li^+ (0.68 Å) than Mn^{4+} (0.60 Å) and Co^{3+} (0.63 Å).

The SEM pictures for different Li-excessive as-prepared materials are shown in Fig. 2. All the samples show analogy morphology with a 5–10 μm particle size approximately, which are comprised of agglomerates of much smaller primary particles. However, with the increasing of Li-excessive value x, the primary particle tends to grow up slightly, even some big primary particles within agglomerates can be distinctly found in $Li_{1.225}Mn_{0.413}Ni_{0.181}Co_{0.181}O_2$ ($x = 0.225$) sample.

The rate capability and cycle performance were tested for $Li_{1+x}(Mn_{0.533}Ni_{0.233}Co_{0.233})_{1-x}O_2$ ($x = 0.045$, 0.09, 0.135, 0.18) materials. The charge and discharge curves in current density of 20, 40, 100 and 200 mA g^{-1} are shown in Figs. 3–6 correspondingly. For the limitation of test facilities, rate capability test exceeding 200 mA g^{-1} is not carried out. Even so, distinct comparison can be obtained in current density of 200 mA g^{-1} or less. At the same time, rate capabilities have been deteriorated to less than 60% (ratio vs. 20 mA g^{-1}) for $Li_{1.135}Mn_{0.461}Ni_{0.202}Co_{0.202}O_2$ ($x = 0.135$) and $Li_{1.18}Mn_{0.438}Ni_{0.191}Co_{0.191}O_2$ ($x = 0.18$) samples in 200 mA g^{-1}, unsuitable for further rate ability testing.

From data shown in Table 2, we can see initial efficiency (Q_{1d}/Q_{1c}) almost keeps the same low-level of 70% for different Li-excessive samples, which can be explained by the irreversible capacity in the first cycle of Li_2MnO_3 for $yLi_2MnO_3{\cdot}(1-y)LiNi_{1/3}Mn_{1/3}Co_{1/3}O_2$ materials. It can also

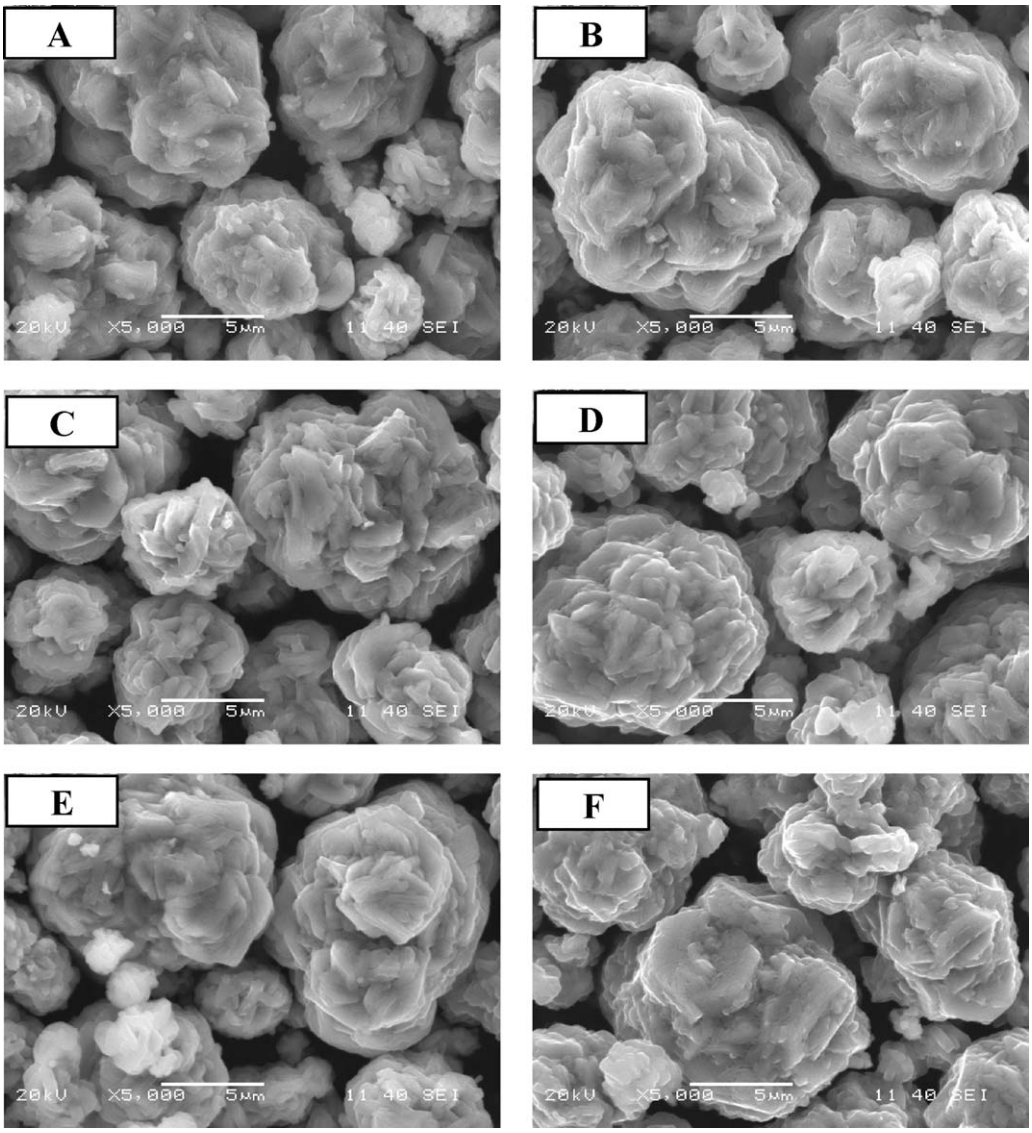

Fig. 2. SEM patterns of $Li_{1+x}(Mn_{0.533}Ni_{0.233}Co_{0.233})_{1-x}O_2$ samples (A, B, C, D, E, E referring to samples of $x = 0$, 0.045, 0.09, 0.135, 0.18, 0.225).

be observed that initial charge voltage plateau of 4.0–4.5 V declined and initial discharge capacity enhanced with the decreasing of Li-excessive, accounting for the increase of relative Li_2MnO_3 amount in $yLi_2MnO_3\cdot(1-y)LiNi_{1/3}Mn_{1/3}Co_{1/3}O_2$ solid solution, resulting in lowest capacity and extreme lower voltage plateau for $Li_{1.18}Mn_{0.438}Ni_{0.191}Co_{0.191}O_2$ sample. Among which the $Li_{1.045}Mn_{0.509}Ni_{0.223}Co_{0.223}O_2$ sample ($x = 0.045$) expresses highest discharge capacity of 259.8 mA h g^{-1}, while the other three samples ($x = 0.09$, 0.135, 0.18) behaves in 250–255 mA h g^{-1}. The initial discharge capacity is relatively high and in accordance with assays reported, where 243.8 mA h g^{-1} in 2.0–4.6 V for $Li[Li_{0.2}Mn_{0.534}Ni_{0.133}Co_{0.133}]O_2$ [13] and 250–265 mA h g^{-1} in 2.0–4.8 V for $Li[Li_{0.2}Mn_{0.54}Ni_{0.13}Co_{0.13}]O_2$ [14]. Yabubuchi et al. viewed that high capacity of $yLi_2MnO_3\cdot(1-y)LiNi_{1/3}Mn_{1/3}Co_{1/3}O_2$ materials after the first charge to high voltage is constituted of redox reaction of Mn^{3+}/Mn^{4+} and oxygen reduction at the electrode surface [15]. Two distinct voltage plateau is observed from the discharge curves, especially for higher Li-excessive samples $Li_{1.135}Mn_{0.461}Ni_{0.202}Co_{0.202}O_2$ and $Li_{1.18}Mn_{0.438}Ni_{0.191}Co_{0.191}O_2$, which corresponding to increase of Li insertion by reduction of Mn^{4+} ion (<3.5 V, region 4 in four charge-discharge region) [16].

When current density rises up to 40 mA g^{-1}, $Li_{1.09}Mn_{0.486}Ni_{0.212}Co_{0.212}O_2$ sample ($x = 0.09$) shows higher discharge capacity of 231.4 mA h g^{-1} and ratio of 90.9%

Table 2
Electrochemical characteristics of $Li_{1+x}(Mn_{0.533}Ni_{0.233}Co_{0.233})_{1-x}O_2$ samples.

x	Q_{1d}/Q_{1c}	Discharge capacity at different rate, mA h g^{-1}				Ratio versus 20 mA g^{-1}, %		
		20 mA g^{-1}	40 mA g^{-1}	100 mA g^{-1}	200 mA g^{-1}	40 mA g^{-1}	100 mA g^{-1}	200 mA g^{-1}
0.045	71.7	259.8	226.1	203.2	177.8	87.0	78.2	68.4
0.090	72.3	254.5	231.4	207.9	186.9	90.9	81.7	73.4
0.135	69.2	251.1	223.4	184.8	146.1	89.0	73.6	58.2
0.180	63.8	250.9	223.3	186.1	134.3	89.0	74.2	53.5

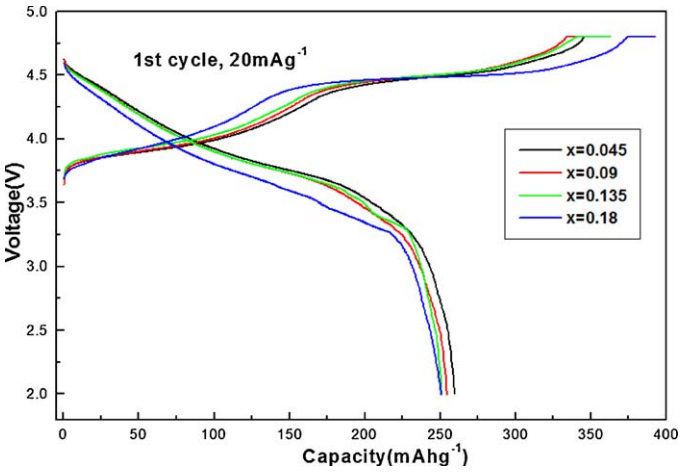

Fig. 3. Initial charge/discharge curves of $Li_{1+x}(Mn_{0.533}Ni_{0.233}Co_{0.233})_{1-x}O_2$ samples at 20 mA g^{-1}.

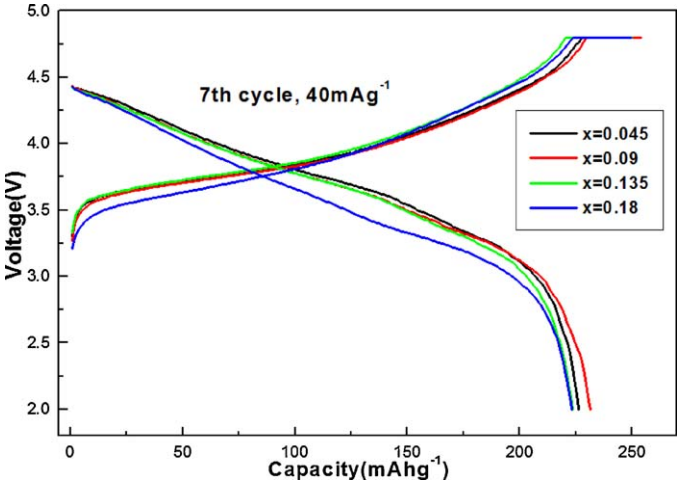

Fig. 4. Initial charge/discharge curves of $Li_{1+x}(Mn_{0.533}Ni_{0.233}Co_{0.233})_{1-x}O_2$ samples at 40 mA g^{-1}.

versus 20 mA g^{-1}, followed by $Li_{1.045}Mn_{0.509}Ni_{0.223}Co_{0.223}O_2$ of 226.1 mA h g^{-1}, $Li_{1.135}Mn_{0.461}Ni_{0.202}Co_{0.202}O_2$ of 223.4 mA h g^{-1}, and $Li_{1.18}Mn_{0.438}Ni_{0.191}Co_{0.191}O_2$ of 223.3 mA h g^{-1}, no obvious distinction is observed for the other three. However, the

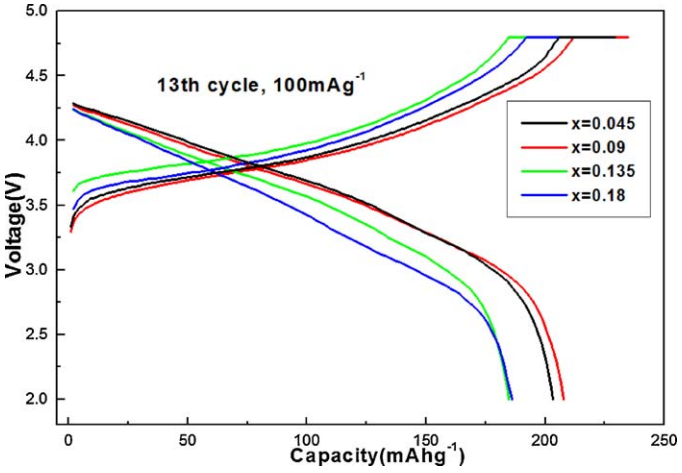

Fig. 5. Initial charge/discharge curves of $Li_{1+x}(Mn_{0.533}Ni_{0.233}Co_{0.233})_{1-x}O_2$ samples at 100 mA g^{-1}.

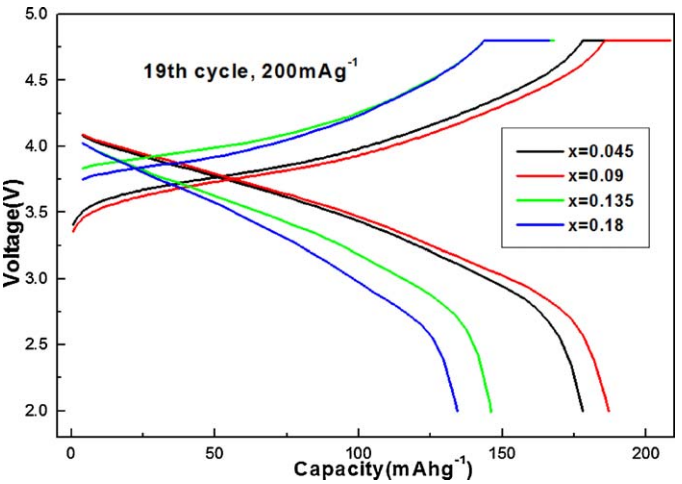

Fig. 6. Initial charge/discharge curves of $Li_{1+x}(Mn_{0.533}Ni_{0.233}Co_{0.233})_{1-x}O_2$ samples at 200 mA g^{-1}.

variation trend becomes distinct in 100 mA g^{-1} and 200 mA g^{-1}. The Li-excessive value x of 0.09 sample exhibits the best rate capability, then sample of 0.045, 0.135 and 0.18 diminishing followed. $Li_{1.09}Mn_{0.486}Ni_{0.212}Co_{0.212}O_2$ sample shows 207.9 mA h g^{-1} (81.7% vs. 20 mA g^{-1}) in 100 mA g^{-1} and 186.9 mA h g^{-1} (73.4% vs. 20 mA g^{-1}) in 200 mA g^{-1}. The rate data are also well accordance with or slightly lower than assays reported. On the other hand, $Li_{1.18}Mn_{0.438}Ni_{0.191}Co_{0.191}O_2$ sample shows lowest capability of 134.3 mA h g^{-1} (53.5% vs. to 20 mA g^{-1}) in 200 mA g^{-1}.

The rate capability and cycle performance for as-prepared materials are presented in Fig. 7. At different discharge rate, almost no reduction is observed after 24-time cycles in all for $Li_{1.09}Mn_{0.486}Ni_{0.212}Co_{0.212}O_2$ sample. In addition, we found the other three samples exhibit poor cycle performance, especially discharged in higher current density for relatively higher Li-excessive samples. Compared to $LiCoO_2$, $LiNi_{1/3}Mn_{1/3}Co_{1/3}O_2$ and other commercial used cathode materials, the as prepared materials present both excellent discharge capacity and cycle performance, but rate capability needs further improvement. Through optimization of Li-excessive amount, rate capability can be improved to some extent by reducing the extent of Li/Ni disorder. It is concluded that both rate and cycle capability behaves better when Li-excessive value x is 0.09 and analysis is supposed as follows. As XRD patterns reveal, when Li-excessive is located in 0 and 0.225, pure phase cannot be obtained. $yLi_2MnO_3{\cdot}(1-y)LiNi_{1/3}Mn_{1/3}Co_{1/3}O_2$

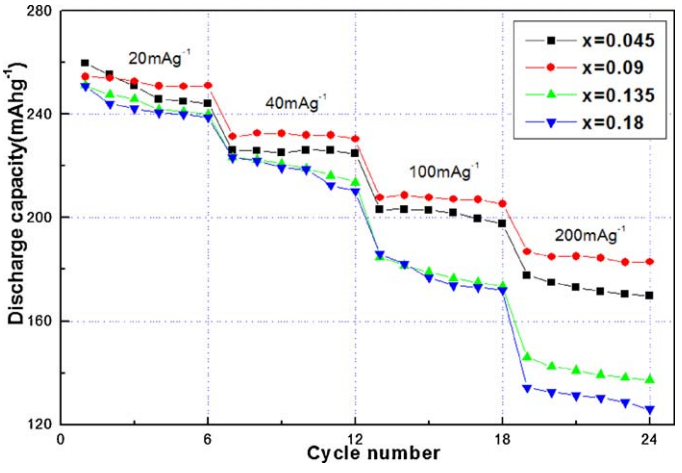

Fig. 7. Cycle ability performance of $Li_{1+x}(Mn_{0.533}Ni_{0.233}Co_{0.233})_{1-x}O_2$ samples.

solid solution comes into being while Li-excessive keeps between 0.045 and 0.18. Furthermore, with the increase of Li content, Li_2MnO_3 phase increases either. Li/Ni disorder occurs when Li content is deficient; residual Li_2MnO_3 exists in outer of $yLi_2MnO_3{\cdot}(1-y)LiNi_{1/3}Mn_{1/3}Co_{1/3}O_2$ solid solution when Li content is abundant. Both the Li/Ni disorder and residual Li_2MnO_3 will deteriorate rate and cycle capability. Maybe Li-excessive value of 0.09 ($Li_{1.09}Mn_{0.486}Ni_{0.212}Co_{0.212}O_2$ sample) is the optimum point. The analogy phenomenon is also presented in our previous research work of $Li_{1+x}(Mn_{0.65*0.995}Ni_{0.35*0.995}Co_{0.005})_{1-x}O_2$ and none-doped $Li_{1+x}(Mn_{0.65}Ni_{0.35})_{1-x}O_2$ cathode materials, in which Li-excessive of 0.0909 is the optimum point. Regretfully, Li/Ni disorder or residual Li_2MnO_3 cannot be detected and verified at present work, which needs to be further lucubrated in later investigation.

4. Conclusions

Li-rich Mn-based $Li_{1+x}(Mn_{0.533}Ni_{0.233}Co_{0.233})_{1-x}O_2$ ($x = 0$, 0.045, 0.09, 0.135, 0.18, 0.225) materials were prepared by a conventional solid-state reaction. Pure phase indexed as a layered oxide structure based on a hexagonal α-$NaFeO_2$ structure can be obtained when Li-excessive value x keeps between 0.045 and 0.18. With the increasing of Li-excessive, the lattice parameters a, c and V have increased but c/a decreased and the primary particle tends to grow up slightly. For the irreversible capacity in the first cycle of Li_2MnO_3, the initial efficiency (Q_{1d}/Q_{1c}) keeps the same low-level of 70% for different samples. $Li_{1.045}Mn_{0.509}Ni_{0.223}Co_{0.223}O_2$ sample ($x = 0.045$) expresses highest initial discharge capacity of 259.8 mA h g^{-1}, while $Li_{1.09}Mn_{0.486}Ni_{0.212}Co_{0.212}O_2$ sample ($x = 0.09$) shows higher discharge capacity of 231.4 mA h g^{-1} in 40 mA g^{-1} and ratio of 90.9% versus 20 mA g^{-1}. The Li-excessive value x of 0.09 sample exhibits the best rate capability in 100 mA g^{-1} and 200 mA g^{-1}. Almost no reduction is observed after 24-time cycles in all for $Li_{1.09}Mn_{0.486}Ni_{0.212}Co_{0.212}O_2$ sample, which reveals the optimum point for $yLi_2MnO_3{\cdot}(1-y)LiNi_{1/3}Mn_{1/3}Co_{1/3}O_2$ solid solution. Research work must be carried out further to verify the Li/Ni disorder and residual Li_2MnO_3.

References

[1] X.-J. Guo, Y.-X. Li, M. Zheng, J.-M. Zheng, J. Li, Z.-L. Gong, Y. Yang, Journal of Power Sources 184 (2008) 414.
[2] L. Yu, W. Qiu, F. Lian, W. Liu, X. Kang, J. Huang, Materials 62 (2008) 3010.
[3] L. Yu, W. Qiu, F. Lian, J. Huang, X. Kang, Journal of Alloys and Compounds 471 (2009) 317.
[4] L.-Y. Yu, W.-H. Qiu, J.-Y. Huang, F. Lian, International Journal of Minerals, Metallurgy and Materials 16 (2009) 458.
[5] Y. Wu, A. Manthiram, Journal of Power Sources 183 (2008) 749.
[6] A. Ito, D. Li, Y. Sato, M. Arao, M. Watanabe, M. Hatano, H. Horiea, Y. Ohsawa, Journal of Power Sources 195 (2010) 567.
[7] J. Li, R. Klopsch, M.C. Stan, S. Nowak, M. kunze, M. Winter, S. Passerini, Journal of Power Sources 196 (2011) 4821.
[8] A. Ito, Y. Sato, T. Sanada, M. Hatano, H. Horie, Y. Ohsawa, Journal of Power Sources 196 (2011) 6828.
[9] Y. Wu, A. Manthiram, Solid State Ionics 180 (2009) 50.
[10] R. Santhanam, P. Jones, A. Sumana, B. Rambabu, Journal of Power Sources 195 (2010) 7391.
[11] A. Ito, K. Shoda, Y. Sato, M. Hatano, H. Horie, Y. Ohsawa, Journal of Power Sources 196 (2011) 4785.
[12] W.C. West, R.J. Santiewicz, C. Ma, J. Robak, J. Soler, M.C. Smart, B.V. Ratnakumar, Journal of Power Sources 196 (2011) 9696.
[13] J.-H. Lim, H. Bang, K.-S. Lee, K. Amine, Y.-K. Sun, Journal of Power Sources 189 (2009) 571.
[14] J.M. Zheng, X.B. Wu, Y. Yang, Electrochimica Acta 56 (2011) 3071.
[15] N. Yabubuchi, K. Yoshii, S.-T. Myung, I. Nakai, S. Komaba, Journal of the American Chemical Society 133 (2011) 4404.
[16] S.-H. Kang, Michael M. Thackeray, Electrochemistry Communications 11 (2009) 748.